THE EFFICIENCY OF THE HEAT PIPE OF KNOWN GEOMETRY USING A NUMBER OF REFRIGERANTS

Grzegorz Górecki*
*Author for correspondence
Institute of Turbomachinery,
Lodz University of Technology,
Lodz, 219/223 Wolczanska Street,
Poland,
E-mail: grzegorz.gorecki@p.lodz.pl

Efficiency of gravity assisted heat pipe (thermosyphon) is studied. Tests were performed for a known geometry of a heat pipe 550 mm long, 22 mm outer diameter and wall thickness of 1 mm. Goal of present research is to determine the influence of phase change process (boiling, condensation) occurring inside the heat pipe for variety of working conditions. The study was conducted for the following refrigerants filling the interior of the heat pipe: R134a, R404A, R407C, and R410A. Different amounts of working fluids are considered. Numerical CFD simulation was performed for one case for validation and better understanding of two-phase processes occurring inside thermosyphon. Efficiency and effectiveness of the heat pipe was calculated on the basis of obtained experimental research data.

INTRODUCTION

The heat pipe consists of three sections: evaporator, adiabatic and condenser. Evaporator is the heated part of a heat pipe. Fluid is evaporating in elevated temperature and pressure conditions. Condenser is heat sink region, where vapor is condensing [1],[2],[3]. Depending on working fluid used, heat pipe can work in wide range of temperatures, from 4 K (helium) to 2500 K (liquid silver). Heat pipe container material and working fluid should be compatible with each other. [1]. Due to different construction two main heat pipe types can be distinguished: with capillary structure and with gravity induced flow [4],[5]. The heat pipe where liquid circulates due gravity force is also called two-phase thermosyphon which is the subject of present study. Two-phase closed thermosyphon gained attention as heat recovery system component. Heat exchangers made of thermosyphons banks are highly efficient air conditioning, flue gas or wastewater heat recovery systems. Low temperature applications include also de-icing, geothermal heating etc. Numerous studies were conducted to obtain throughput of refrigerant filled, "wickless" heat pipes at low temperature conditions dedicated for mentioned recuperation systems. Refrigerants exhibits higher overall conductance and throughputs than water or alcohols used usually as working fluids (in considered temperature range). From so called modern refrigerants R134a gained most attention in research as heat pipe working fluid [6], [7], [8]. R410A was also tested as medium in rotating heat pipes [9]. Yet, there hasn't been comprehensive and comparative study of modern refrigerants as working fluids of two-phase closed thermosyphons. Present work tries to complement previous studies, comparing thermal performance of heat pipe filled with R134a, R404A, R407C and R410A. The best refrigerant could be used as working fluid in recuperation or passive low-temperature systems.

NOMENCLATURE

c_p	[J/kg K]	Constant pressure heat capacity
U	[mV]	Voltage
FR	[%]	Filling ratio
K	[K/mV]	Thermocouple constant
p	[bar/Pa]	Pressure
T	[K]	Temperature
V	[m^3]	Volume
$\dot{V}$	[m^3/s]	Volumetric flow rate
$\dot{Q}$	[W=J/s]	Heat flow rate
ρ	[kg/m^3]	Density
α	[-]	Volume fraction
μ	[Pa s]	Dynamic viscosity
δij		Kronecker delta
E	[J/kg]	Total energy per unit mass
q	[W/m^2]	Conductive heat flux
S_E	[W/m^3]	Energy source
S_F	[kg/m^{2}s^2]	Momentum source
S_M	[kg/m^{3}s]	Mass source
u	[m/s]	Velocity component
t	[s]	time

Special characters

Δ	[-]	Difference

Subscripts

1	Inlet
2	Outlet
C	Cold water

l	liquid
h	Hot water
r	Refrigerant
t	Thermosyphon
v	Vapor
a	Mean value
R134a	Refrigerant R134a
R404A	Refrigerant R404A
R407C	Refrigerant R407C
R410A	Refrigerant R410A

EXPERIMENTAL SETUP

Tested heat pipe is made from brass. Measurements were carried for known geometry: 550mm length, outer diameter - 22mm and wall thickness - 1mm. It was charged with varying amounts: 10, 20, 30 and 40% of its whole internal volume, with modern refrigerants: R134a, R404A, R407C and R410A. These refrigerants were chosen because of frequent use in industry (their popularity). The heat pipe was enclosed by two stainless steel heat exchangers, one on the evaporator section and second on the condenser section. Whole assemble was thermally insulated to limit environment influence on measurements. Water was fed into heat exchangers. Stream of water flowing into bottom heat exchanger, heating the evaporator section, was kept at steady and fixed temperature level varying from 288 K to 323 K. Water fed into top heat exchanger was at constant temperature level of 283 K, cooling the condenser section.

During measurements steady volumetric flow of water was provided by adjusting regulation valves. Two constant temperature baths operate with chiller that maintains constant inlet temperatures of hot and cold water. Hot water temperature was increased by 5 K in the range of 288 to 323 K. Measurements were read after thermal stabilization of the system (steady state). The two-phase thermosyphon was filled with self-constructed, high precision charging system.

Thermoelectrical force was measured at chosen points on heat pipe surface, as well as inlet and outlet (positions depicted in Figure 1).

Pressure inside thermosyphon was also measured, and saturation temperature of working fluid was found from tables. Pressure inside the heat pipe is of great importance. On the basis of the pressure, saturation temperature is determined and performance of the system is evaluated. The heat pipe performance depends on saturation temperature inside it and on the value of hot water temperature at the inlet to bottom heat exchanger. Heat pipe performs well when inlet water temperature is considerably higher than saturation temperature inside. Figure 2 presents experimental rig. Apart from mentioned constant temperature heat baths, chiller and high precision (1% filling ratio accuracy) charging system, regulation valves were used for controlling the flow rate. Flow rate was measured by rotameters and impulse flow transducers. Thermoelectric force from thermocouples was measured by milivoltmeter and plotted by measurements recorder. Inside thermosyphon pressure was measured directly from one of Schreder valves on the charging system. Part of charging system pressure was always in equilibrium with inside thermosyphon pressure. Pressure transducer converted pressure for electrical signal read from pressure meter.
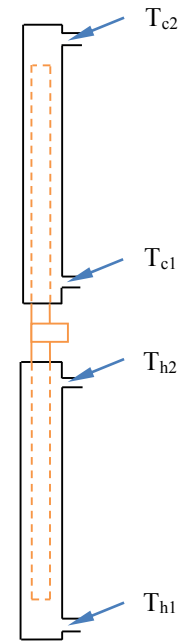

Figure 1 Schematic drawing of the heat pipe assembly with specification of thermoelectrical force measurement sites (temperature): T_{h1} –inlet hot water temperature, T_{h2} –outlet hot water temperature, T_{c1} –inlet cold water temperature, T_{c2} – cold water outlet temperature

Uncertainty analysis was done according to GUM guide [10]. Standard uncertainty for heat transfer rates was determined and turned out to be as high as 5-12 W. For relative combined standard uncertainty on constant level about 8-10%.
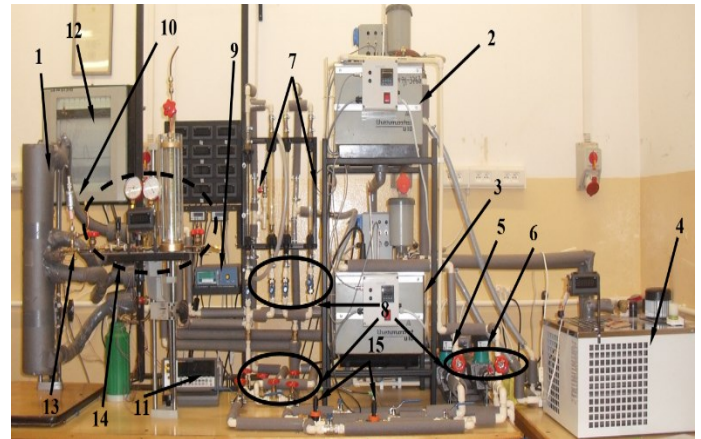

Figure 2 Test rig: 1 – heat pipe with heat exchangers (insulated), 2 – constant temperature cold water bath, 3 – constant temperature hot water bath, 4 – chiller, 5 – hot water pump, 6 – cold water pump, 7 – rotameters, 8 – cut-off and regulation valves 9 – pressure meter 10 –pressure transducer, 11 – milivoltmeter, 12 –measurements recorder, 13 –charging terminal, 14 –high precision charging system, 15 - impulse flow transducers

CALCULATION PROCEDURE

Performance and efficiencies of thermosyphon were obtained by following calculations:
-first water inlet and outlet temperatures are obtained from thermoelectrical force:

$$T = E \cdot K \qquad (1)$$

-heat flow rate from hot water to evaporator:

$$\dot{Q}_h = \Delta T_h \cdot \dot{V}_h \cdot \rho_h \cdot c_{ph} \qquad (2)$$

-heat transfer rate from condenser section to cooling water:

$$\dot{Q}_c = \Delta T_c \cdot \dot{V}_c \cdot \rho_C \cdot c_{pc} \qquad (3)$$

- the heat pipe efficiency:

$$\eta = \frac{\dot{Q}_c}{\dot{Q}_h} \cdot 100 \qquad (4)$$

-filling ratio:

$$FR = \frac{V_r}{V_t} \cdot 100$$

, where V_r - volume of refrigerant, V_t – thermosyphon inside volume

EXPERIMENTAL RESULTS

Figure 3 ÷ Figure 6 represent respectively heat transfer rates from hot water to the evaporator, heat transfer rates from the condenser to cold water, heat pipe efficiency and inside pressure versus approximate temperature of hot water at inlet for the thermosyphon filled with different amount of R134a refrigerant.
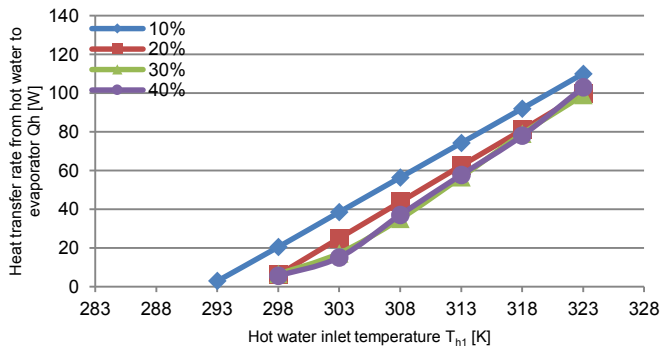
Figure 3 Heat transfer rates from hot water to evaporator for various filling ratios of thermosyphon charged with R134a refrigerant versus approximate hot water inlet temperature
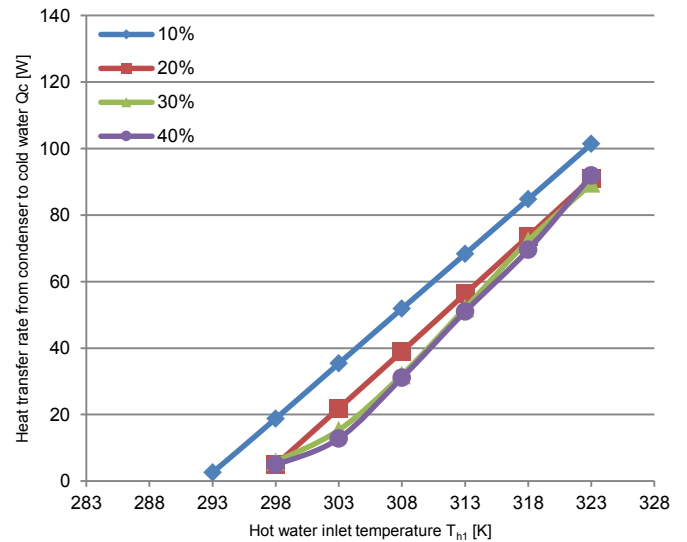

Figure 4 Heat transfer rates from condenser to cold water for various filling ratios of thermosyphon charged with R134a refrigerant versus approximate hot water inlet temperature

The heat pipe charged with R134a refrigerant performed efficiently (there was no limits present) starting from 293 K temperature, for 10% filling ratio, and for the rest of considered FR range it performed well. The heat pipe doesn't work properly below 293 K for 10%. It can be recognized by low heat fluxes and elevated evaporator wall temperature. For R134a refrigerant the highest heat transfer rates and efficiencies are obtained for 10% volumetric ratio. Heat transfer rate from hot water to evaporator was 110 W, and from the condenser to cold water approximately 101 W. Throughput for this filling ratio was 90 ÷ 92 W.
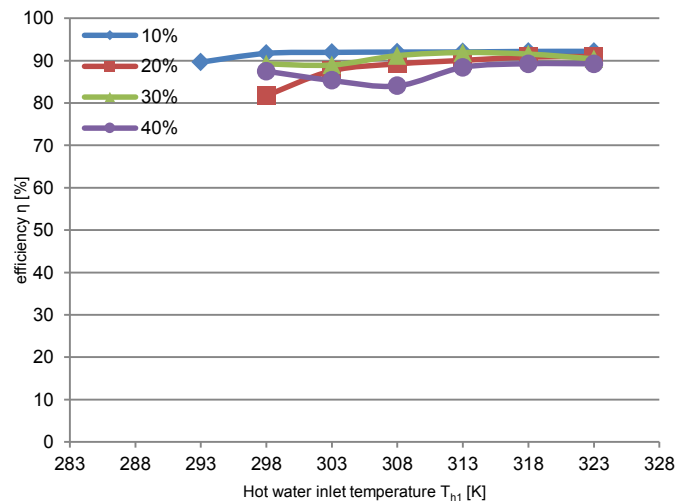

Figure 5 Efficiency for various filling ratios of thermosyphon charged with R134a refrigerant versus approximate hot water inlet temperature
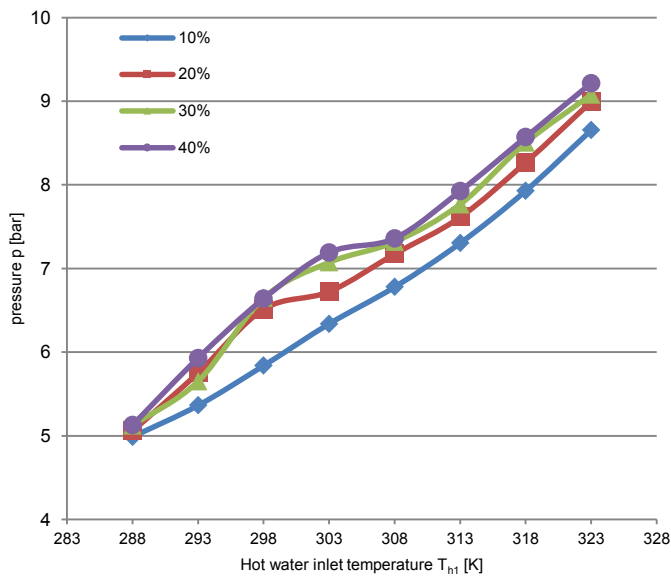
Figure 6 Pressure inside thermosyphon for various filling ratios with R134a refrigerant versus approximate hot water inlet temperature

The lowest values of heat transfer rates were measured for 30% and 40% filling ratio. The lowest values of efficiency was reported for 20 and 30% whole volume of the heat pipe charged with refrigerant. The highest heat pipe throughput was reached with 10% filling ratio for R134a refrigerant. The least effective were 30 and 40% ratios. Along with increase in inlet hot water temperature, pressure inside the heat pipe was increasing. The highest inside pressure was reported for 40% filling ratio. For 10% inside pressure was the lowest.

Figure 7 ÷ Figure 10 show respectively: heat transfer rate from hot water to evaporator, heat transfer rates from condenser to cold water and inside pressure versus approximate hot water inlet temperature for thermosyphon charged with R404A refrigerant. Heat pipe started to perform properly from 298K hot water inlet temperature for thermosyphon filling ratio with R404A refrigerant for 30% and 40% its total volume, in other cases heat pipe was operating properly in whole range. Heat transfer rates from hot water to the evaporator and from the condenser section to cold water were for 20%, 30% and 40% filling ratio. The lowest heat transfer rate was reported for 10% filling ratio.

The highest efficiency were obtained for 30% filling ratio and „stayed" at virtually steady level of 85 ÷ 86%. The lowest efficiency was observed for 10% filling ratio. Taking heat transfer ratio into account the heat pipe worked most effectively for 20%, 30% and 40% filling ratio for R404A refrigerant. The least effective filling ratio was 10%.
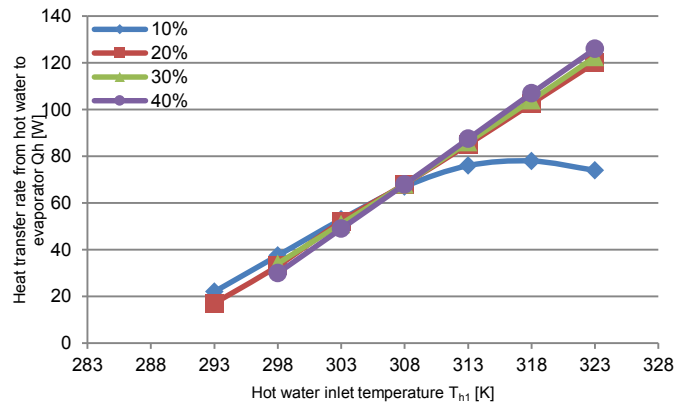

Figure 7 Heat transfer rates from hot water to evaporator for various filling ratios of thermosyphon charged with R404A refrigerant versus approximate hot water inlet temperature
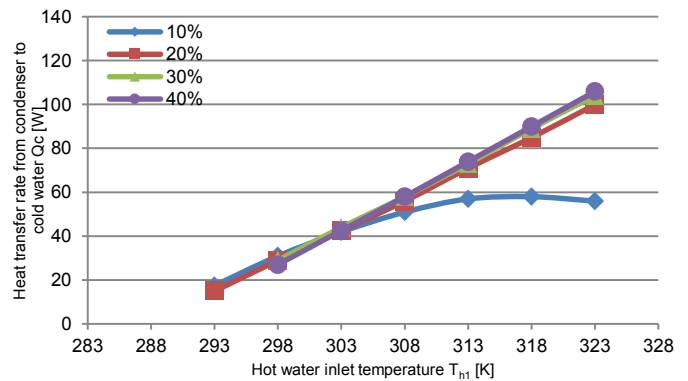

Figure 8 Heat transfer rates from condenser to cold water for various filling ratios of thermosyphon charged with R404A refrigerant versus approximate hot water inlet temperature
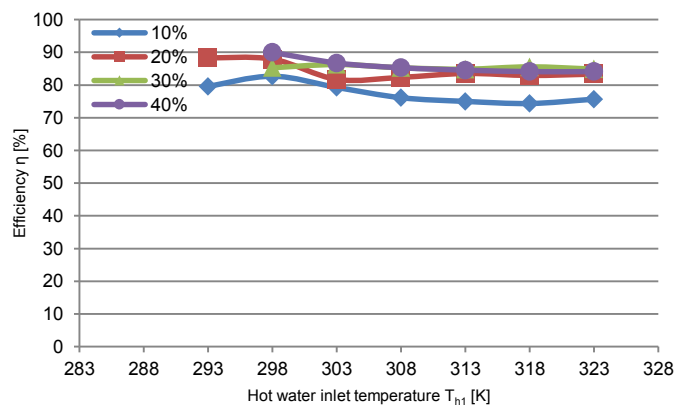

Figure 9 Efficiency for various filling ratios of thermosyphon charged with R404A refrigerant versus approximate hot water inlet temperature
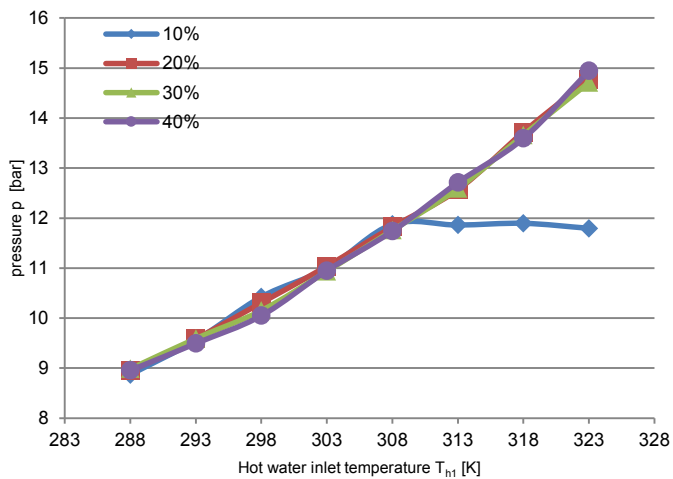
Figure 10 Pressure inside thermosyphon for various filling ratios with R404A refrigerant versus approximate hot water inlet temperature

Inside pipe pressure increased linearly with raising hot water inlet temperature. Pressures for filling ratios 20%, 30% and 40% were virtually identical. For 10% filling ratio, above 308K temperature, pressure stayed approximately at a constant level. It was caused by thermosyphon operation limit called dryout limit. Pressure will not increase during the limit because boiling heat transfer coefficient deteriorates.

In Figure 11 ÷ Figure 14 are presented respectively: heat transfer rates from hot water to evaporator, heat transfer rates from condenser to cold water and thermosyphon thermal efficiency,versus hot water inlet temperature for the thermosyphon charged with R407C refrigerant.
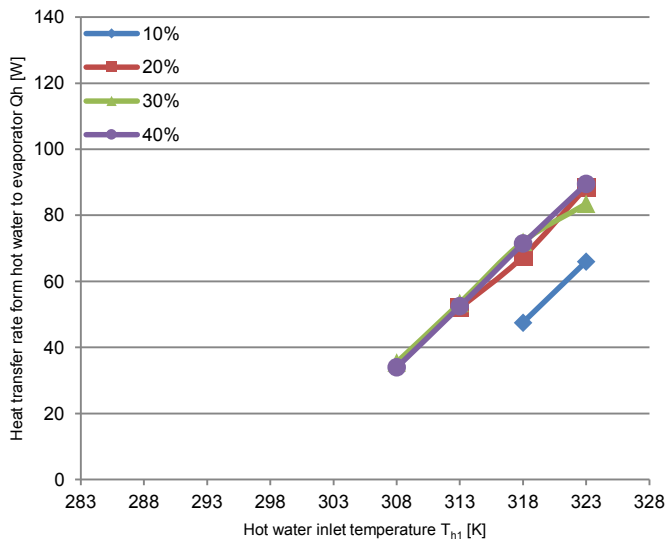

Figure 11 Heat transfer rates from hot water to evaporator for various filling ratios of thermosyphon charged with R407C refrigerant versus approximate hot water inlet temperature
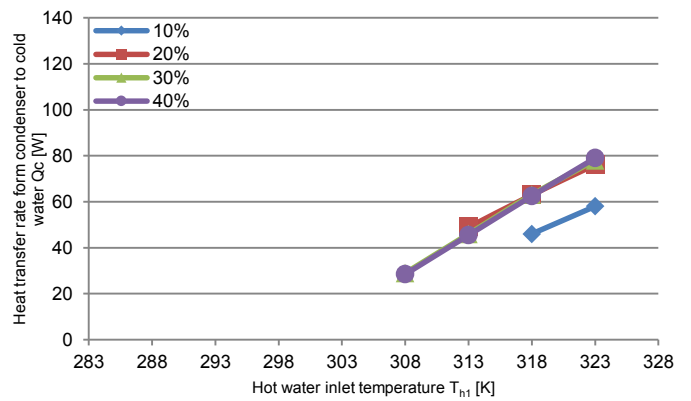

Figure 12 Heat transfer rates from condenser to cold water for various filling ratios of thermosyphon charged with R407C refrigerant versus approximate hot water inlet temperature
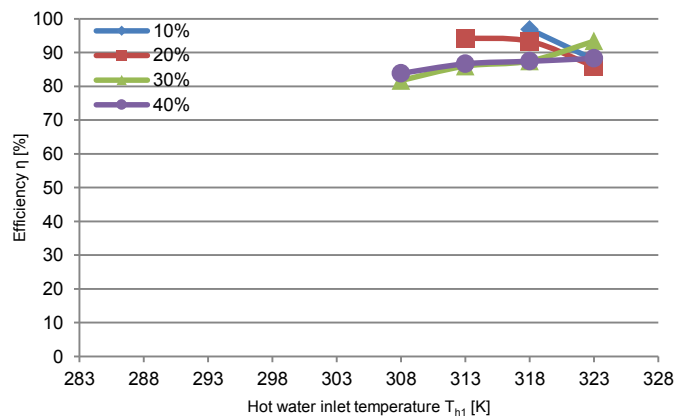

Figure 13 Efficiency for various filling ratios of thermosyphon charged with R407C refrigerant versus approximate hot water inlet temperature
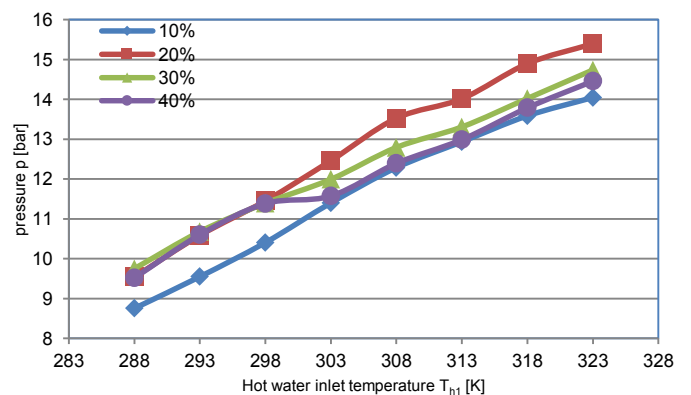

Figure 14 Pressure inside thermosyphon for various filling ratios with R407C refrigerant versus approximate hot water inlet temperature

The heat pipe charged with R407C refrigerant for 30 and 40% filling ratio operates properly from 308 K, and decrease for smaller filling ratios.

For every filling ratio, heat transfer rates from hot water to evaporator and from condenser to cold water are comparable, excluding 10% filling ratio for which dryout limit occurs.

The highest efficiency reported for the heat pipe was for 10% filling ratio, however the thermosyphon operation range is very narrow. The lowest efficiencies were obtained for 30% - 40% filling ratio, but it corresponds to wider operation range.

The heat pipe charged with R407C refrigerant worked most effectively for 30% and 40% filling ratio. The least effective filling ratio was 10%.

Pressure inside thermosyphon increase linearly. The highest inside pressure was measured for 20% filling ratio. Lowest value of pressure was noted for 10%. Inside pressure increased proportionally to hot water inlet temperature.

In Figure 15 ÷ Figure 18 respectively heat transfer rates from hot water to the evaporator, heat transfer rates from the condenser to cold water, heat pipe efficiencies and inside pressure from hot water inlet temperature for thermosyphon R410A refrigerant .
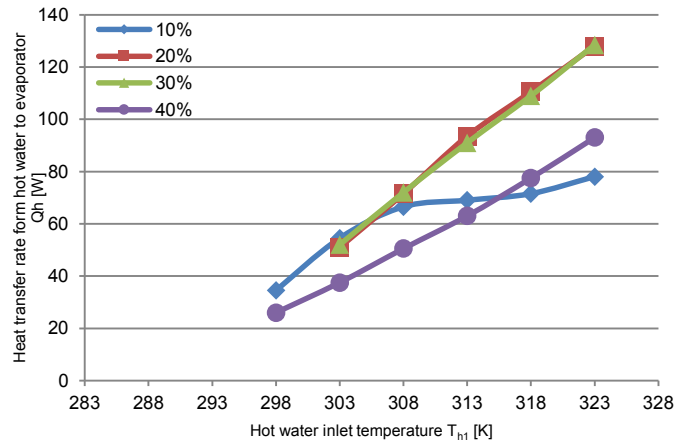

Figure 15 Heat transfer rates from hot water to evaporator for various filling ratios of thermosyphon charged with R410A refrigerant versus approximate hot water inlet temperature
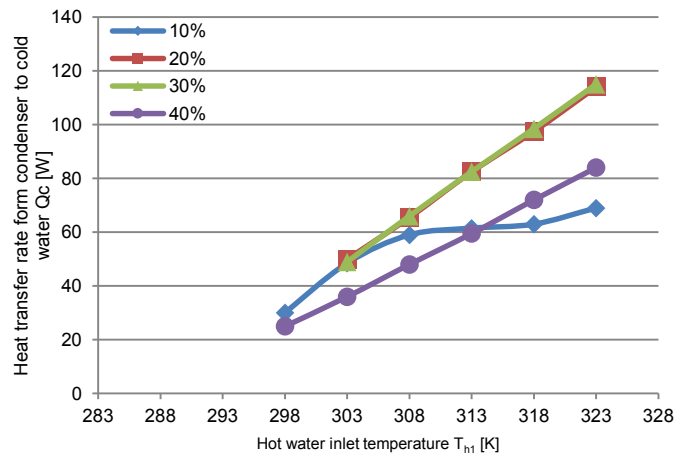

Figure 16 Heat transfer rates from condenser to cold water for various filling ratios of thermosyphon charged with R410A refrigerant versus approximate hot water inlet temperature
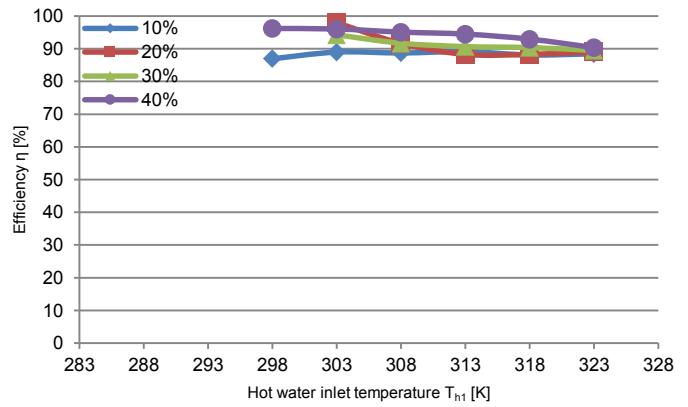

Figure 17 Efficiency for various filling ratios of thermosyphon charged with R410A refrigerant versus approximate hot water inlet temperature
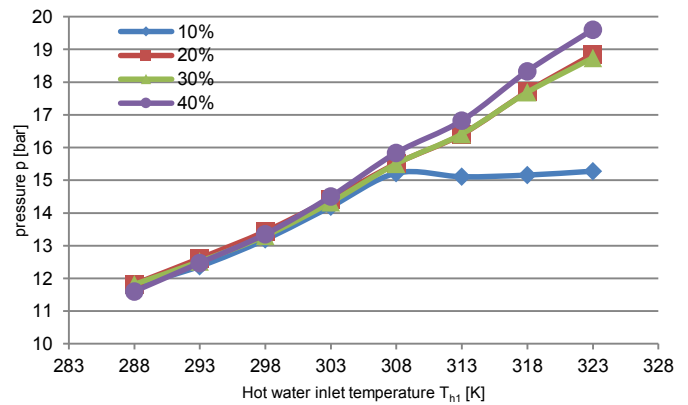

Figure 18 Pressure inside thermosyphon for various filling ratios with R410A refrigerant versus approximate hot water inlet temperature

Thermosyphon filled with R410A refrigerant, for 10% and 40% filling ratio started to operate properly from 298 K, for 20% and 30% from 303 K. The highest heat transfer rates from hot water to evaporator and from condenser to cold water were reported for 20% and 30% filling ratio. The lowest heat transfer rates occurs for 40% and 10%. The highest efficiencies was obtained for 40% filling ratio, the lowest for 10% filling ratio.

Most effective filling ratios for R410A refrigerant were 20 and 30%. The least effective are respectively 10 and 40% filling ratios.

Thermosyphon inside pressure increases linearly for every filing ratio, excluding 10%. For which from 308K temperature operation limit occurs. The highest heat pipe inside pressure was obtained for 40% filling ratio.

CFD SIMULATION

For CFD simulation single case was chosen (one filling ratio and inlet temperatures) where thermosyphon was charged with R410A refrigerant and filling ratio was 30%. Inlet hot water temperature was 323 K. Inlet cold water temperature was 283 K. Temperatures measured on heat pipe outer wall were presented in Table 1. On the basis of this data numerical

simulation was validated. Reported heat transfer coefficients from cold and hot water was comparable and their values were about 700 W/(m² K). Mean throughput was 121.5 W.

Temp.[K]	309	306.5	304	302.5	301.5	298	298.5	299.5
Position[m]	0.02	0.09	0.16	0.26	0.29	0.39	0.46	0.53

Table 1 Measured temperatures at longitudinal positions (from bottom of the heat pipe)

Flow and heat transfer inside thermosyphon was simulated in ANSYS FLUENT program by similar approach like in [12]. Program's solver solved Navier-Stokes equations that can be written as:

Continuity equation:

$$\frac{\partial}{\partial t}(\rho) + \sum_{j=1}^{3}\frac{\partial}{\partial x_j}(\rho u_j) = S_M \qquad (5)$$

Momentum:

$$\frac{\partial}{\partial t}(\rho u_i) + \sum_{j=1}^{3}\frac{\partial}{\partial x_j}(\rho u_i u_j) = -\frac{\partial p}{\partial x_i} + \sum_{j=1}^{3}\frac{\partial}{\partial x_j}\left[\mu\left(\frac{\partial u_i}{\partial x_j} + \frac{\partial u_j}{\partial x_i} - \frac{2}{3}\delta_{ij}\sum_{j=1}^{3}\frac{\partial u_i}{\partial x_i}\right)\right] + S_{F,i} \quad (6)$$

Energy:

$$\frac{\partial}{\partial t}(\rho E) + \sum_{j=1}^{3}\frac{\partial}{\partial x_j}(\rho E u_j) = \sum_{i=1}^{3}\sum_{j=1}^{3}\left(\frac{\partial}{\partial x_j}(\tau_{ij})u_i\right) - \sum_{j=1}^{3}\frac{\partial}{\partial x_j}q_j + S_E \qquad (7)$$

Multiphase flow was solved with the use of VOF (Volume Of Fluid) method, where two phases were present (liquid and vapor). Thermophysical properties are weighted average, where weighting factor is volume fraction α, for example:

$$\rho = \alpha_v \cdot \rho_v + \alpha_l \cdot \rho_l \qquad (8)$$

$$\alpha_v + \alpha_l = 1 \qquad (9)$$

Energy and temperature is mass averaged. Special algorithm is used for interface tracking/reconstruction (Geo-Reconstruct). For more detailed description of VOF method reader should refer to [11]. Transient simulation was carried on until approximate steady state was reported. In Figure 19 initial volume fraction distribution is shown (30% filling ratio). Small vapor chunks were visible near wall inside liquid pool.(Figure 20). This chunks represent bubble aggregates produced in boiling process. Bubbles volume is relatively low, because of high R410A vapor density (even enthalpy of vaporization is considerably smaller – compared to water). For condenser section very thin liquid film or liquid structures falling are recognized (drop like). In Figure 21 velocity distribution near the wall at condenser section is showed. Conclusion of CFD simulation is presented in Figure 22. Measured wall temperature along thermosyphon is compared to temperature obtained from CFD simulation. Yellow line represents measured temperatures, red (evaporator section), white (adiabatic section), and green points (condenser section) represent simulation results. Deviation from real condenser

section temperature is relatively small (1 K at most). Simulation reports greater differences with experimental values at evaporator section (about 5 K at the bottom of evaporator section). There is also visible disagreement between temperature distributions along evaporator. It is caused by thinner than, occurring in reality liquid film, that is broken (not continue) in part of evaporator section. It can be seen in Figure 22 that temperatures at upper part of evaporator section are raised. It is non-physical result of simulation, because heat transfer coefficients should be higher in case of thin film evaporation or boiling than pool boiling.
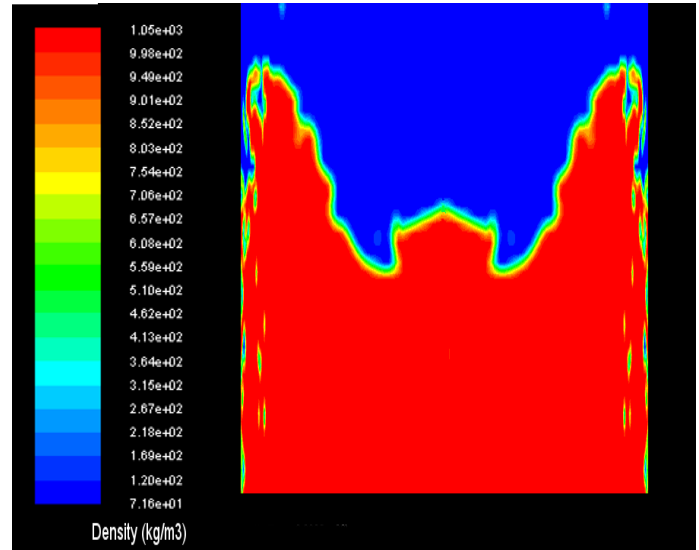

Figure 19 Density contours near vapor liquid interface, vapor chunks from boiling visible near the wall
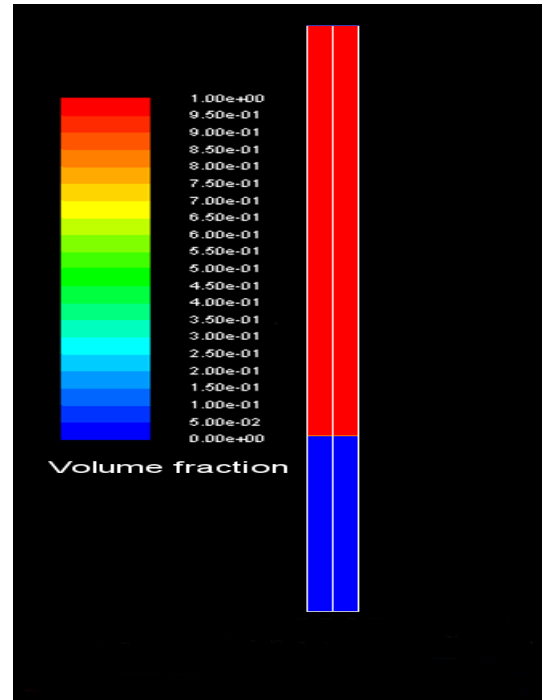

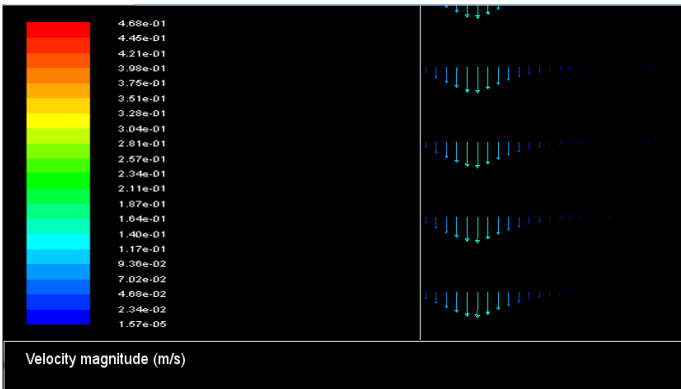**Figure 20** Initial conditions for simulation – 30% filling ratio

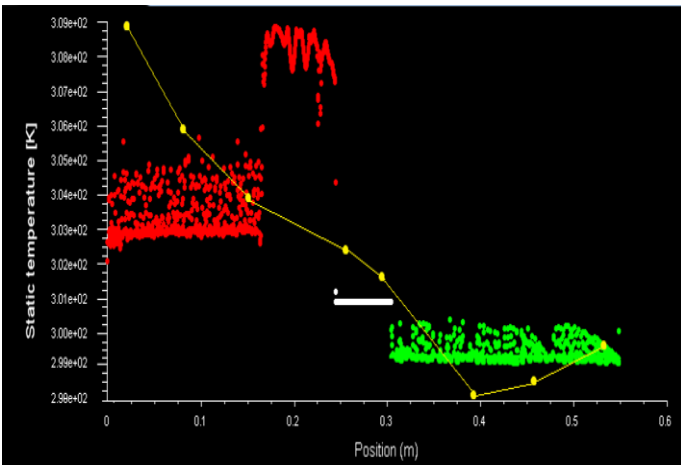**Figure 21** Velocity vectors near the wall (falling liquid film)

Figure 22 Comparison of measured temperatures along thermosyphon (yellow line) and temperatures obtained from CFD simulation

CONCLUSIONS

On the basis of present experimental results for every refrigerant (working fluid) the best filling ratio (highest throughput) was chosen. Also the most effective refrigerant was chosen. Comparison of reported heat transfer rates, from hot water to evaporator and from condenser to cold water and inside pressure were shown in Figure 23 ÷ Figure 26. For R134a refrigerant 10% filling ratio (the best) was chosen, for R404A – 20%, R407C – 30% and R410A – 30%. The highest heat transfer rates from hot water to evaporator and heat transfer rates from condenser to cold water were obtained for R410A refrigerant as working fluid for the 30% filling ratio. Even the throughput using R410A is the highest, drawback is narrow operation range (from 308 K to 323 K). For 30% filling ratio of R410A refrigerant CFD simulation was conducted. Results show good agreement at condenser section but more deviation from experimental data at evaporator section. The main reason is not physical simulation of falling liquid film boiling/evaporation. Similar throughputs (a little lower) were reported for R404A refrigerant for 20% filling ratio. Advantage of second refrigerant is wider operation range (from 293 K to 323 K) and lower inside pressure than R410A for about 3÷4 bar. This fact makes R404A refrigerant the best selection.
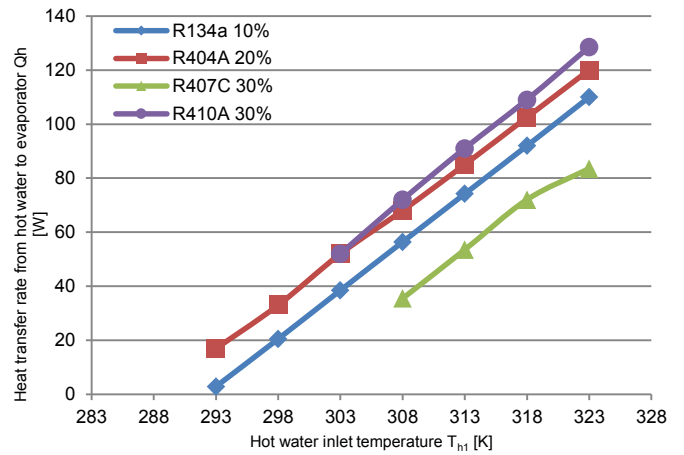

Figure 23 Heat transfer rates from hot water to evaporator for the best filling ratios for every of refrigerants versus approximate hot water inlet temperature
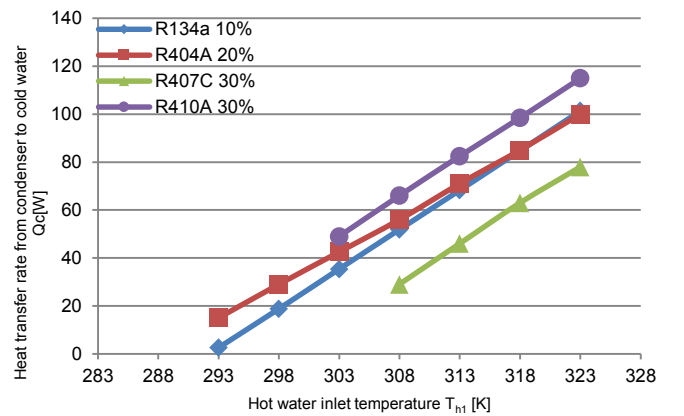

Figure 24 Heat transfer rates from condenser to cold water for the best filling ratios for every of refrigerants versus approximate hot water inlet temperature
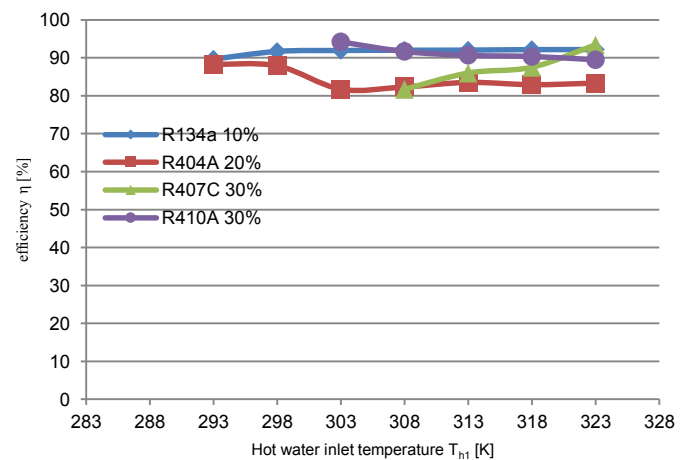

Figure 25 Thermal efficiencies for the best filling ratios for every of refrigerants versus approximate hot water inlet temperature
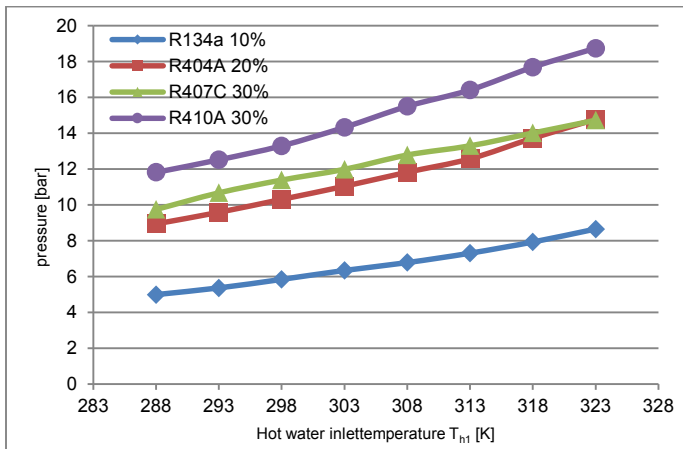
Figure 26 Inside pressure in thermosyphon for the best filling ratios for every refrigerant versus approximate hot water inlet temperature

REFERENCES

[1] Reay D.A., Kew P.A, *Heat Pipes. Theory, Design and Applications*. Butterworth-Heinemann, pp. 1-2, 107-112, 275-314 (2006)

[2] Kutz M., *Energy and Power. Mechanical Engineers' Handbook Third Edition*, John Wiley & Sons, INC, pp. 335-336, (2006)

[3] Bejan A. and Kraus A.D., *Heat Transfer Handbook,* John Wiley & Sons pp. 1182-1184, (2003)

[4] Adrian Ł.: *Budowa i zasada działania rurek ciepła*, Chłodnictwo&klimatyzacja, 3/2010

[5] Jakóbowski P.: :*Budowa, działanie i zastosowanie rurki ciepła cz.,1,* TChK, 3/2009

[6] Ong K. S., Haider-E-Alahi Md., *Performance of a R-134a-filled thermosyphon*, Applied Thermal Engineering, 23 (18) (2003), pp. 2373-2381

[7] Abou-Ziyan H. Z., Helali A., Fatouh M., Abo El-Nasr M. M., *Performance of stationary and vibrated thermosyphon working with water and R134a*, Applied Thermal Engineering, 21 (8) (2001), pp. 813-830

[8] Payakaruk T., Terdtoon P., Ritthidech S., *Correlations to predict heat transfer characteristics of an inclined closed two-phase thermosyphon at normal operating conditions*, Applied Thermal Engineering, 20 (9) (2000), pp. 781-790

[9] Yau Y. H., Foo Y. C., Comparative study on evaporator heat transfer characteristics of revolving heat pipes filled with R134a, R22 and R410A, International Communications in Heat and Mass Transfer 38 (2) (2011), pp. 202-211

[10] Joint Committee for Guides in Metrology *Evaluation of measurement data - Guide to the expression of uncertainty in measurement* 2008

[11] Hirt C.W., Nichols B.D., *Volume of Fluid (VOF) method for the dynamics of free boundaries*, Journal of Computational Physics, 39 (1) (1981), pp. 201–225

[12] Alizadehdakhel A., Rahimi M., Abdulaziz A., *CFD modeling of flow and heat transfer in a thermosyphon,* International Communications in Heat and Mass Transfer, 37 (3) (2010), pp. 312-318